Published in final edited form as:
Nano Lett. 2010 July 14; 10(7): 2296–2302. doi:10.1021/nl903518f.

Uptake and distribution of ultra-small anatase TiO_2 Alizarin red S nanoconjugates in *Arabidopsis thaliana*

Jasmina Kurepa[*,1], **Tatjana Paunesku**[*,2], **Stefan Vogt**[3], **Hans Arora**[2], **Bryan M. Rabatic**[4], **Jinju Lu**[2], **M. Beau Wanzer**[2], **Gayle E. Woloschak**[#,2], and **Jan A. Smalle**[#,1]
Plant Physiology, Biochemistry, Molecular Biology Program, Department of Plant and Soil Sciences, University of Kentucky, Lexington, Kentucky 40546, Department of Radiation Oncology, Feinberg School of Medicine, Northwestern University, Chicago, IL 60611, X-Ray Science Division, Advanced Photon Source, Argonne National Laboratory Argonne, IL 60439

Abstract

While few publications have documented the uptake of nanoparticles in plants, this is the first study describing uptake and distribution of the ultra-small anatase TiO_2 in the plant model system Arabidopsis. We modified the nanoparticle surface with Alizarin red S and sucrose, and demonstrated that nanoconjugates traversed cell walls, entered into plant cells, and accumulated in specific subcellular locations. Optical and X-ray fluorescence microscopy co-registered the nanoconjugates in cell vacuoles and nuclei.

Keywords

Anatase TiO_2 nanoparticles; TiO_2 nanoconjugates; Arabidopsis thaliana; X-ray fluorescence microscopy (XFM)

The application of nanotechnology to plant systems has lagged behind nanomedicine and nanopharmacology in spite of its potential to generate new tools for the delivery of fertilizers, herbicides and insecticides[1], new ways to manipulate plant genomes[2] and new methods to capture and isolate plant natural products. Compared to the thousands of studies describing the uptake and trafficking of nanoparticles (NPs) in biological systems other than plants, less than twenty reports discussed NP uptake by plant species.[1-16] These studies involved different plant species and different types of NPs which were delivered to intact plants, dissected plant organs or protoplasts using a wide range of application methods. [1-16] Despite the absence of systematic analyses, it has been determined that plants can take up NPs from the environment and transport them through the vascular system to various shoot organs.[4, 9, 15] However, little is known about the uptake mechanisms involved or the subcellular localization and distribution of the internalized NPs.[16] Uptake efficiency has also

[#] Corresponding authors: Prof. G. E. Woloschak, Departments of Radiation Oncology, Radiology, and Cell and Molecular Biology, Northwestern University, Feinberg School of Medicine, Chicago, IL 60611 (USA), g-woloschak@northwestern.edu. Prof. J. A. Smalle, Department of Plant and Soil Sciences, University of Kentucky, Lexington, KY 40546 (USA), jsmalle@uky.edu..
[*]These authors contributed equally to this work.
[1]Department of Plant and Soil Sciences, University of Kentucky, Lexington, KY 40506
[2]Department of Radiation Oncology, Feinberg School of Medicine, Northwestern University, Chicago, IL 60611
[3]X-Ray Science Division, Advanced Photon Source, Argonne National Laboratory, Argonne, IL 60439
[4]Rush Medical College, Chicago, IL 60612

SUPPORTING INFORMATION:
Supporting figures describe AFM and TEM determination of the size and appearance of NPs used in this study (Figure S1), and show additional data describing NC distribution and localization in roots, hypotocyls and cotyledons (Figures S2, S3 and S4). This material is available free of charge via the Internet at http://pubs.acs.org.

not been systematically studied, but it appears to depend on the size and type of NP.[5] Although negative, positive, and even protective effects of NPs on plant growth have been reported [1-15, 17-19], overall, no systematic studies have been conducted to determine the toxic effects of NP on plants and the ecological consequences of plant NP uptake. For example, while the toxicity of metal oxide NPs in animal cells and whole organisms was shown to depend on the NP surface area or dispersity, [20, 21] no similar work was attempted in plants.

Here, we report on the uptake and localization of anatase titanium dioxide (TiO_2) NPs smaller than 5 nm in the plant model system *Arabidopsis thaliana*. We chose to study the Col-0 accession because this is the most commonly used ecotype within the Arabidopsis research community.[22] The numerous resources developed for this genetic background [23, 24] will not only facilitate future analyses of the molecular mechanisms of uptake, intracellular localization and trafficking of NPs, but will also provide opportunities for NP-mediated manipulations of the Arabidopsis genome. In addition, the well-characterized Arabidopsis null mutants and overexpression lines for enzymes of various biochemical pathways offer the possibility for the targeted *in planta* chemical modification of NP surface with pathway intermediates.

TiO_2 NPs are among the most studied NPs to date due to their unique photocatalytic and structural properties, and their capacity to be modified by biologically active molecules such as oligonucleotides, peptides and peptide-nucleic acids. [25-31] Anatase TiO_2 crystals smaller than 20 nm exhibit so called “surface defects” that lead to an increased surface reactivity of NPs [26]. For example, they avidly bind enediol ligands such as dopamine and Alizarin red S (ARS), [27, 29] while phosphates and linear carbon molecules carrying hydroxyl groups form less stable bonds with the NP surface[30]. While enediol ligands are not abundant in animal cells, they are frequent among plant polyphenols, and it may be hoped that TiO_2 NPs such as the ones used in this work may be useful for nano-harvesting (for example, in gathering polyphenols on their surface as they traverse plant cells).

TiO_2 NPs with average diameters of 2.8 ± 1.4 nm and NP dispersity of 43% (see Supporting information) were synthesized by a low-temperature alkaline hydrolysis route as described previously [29], and were dialyzed and stored at 4°C in a 10 mM Na_2HPO_4 pH 5.7 buffer. For more detailed information about these NPs and atomic force and TEM micrographs, please see the Supporting Information and Figure S1. A batch of NPs was further modified by dialysis in a 10 mM Na_2HPO_4 pH 5.7 buffer supplemented with 1 M sucrose. Under such conditions, NP surface sites become saturated with sucrose making them less reactive with different types of sugars present in plants.

We have recently described a simple method for the labeling of TiO_2 NPs with ARS which allows their intracellular detection using both bright-field and fluorescent microscopy, and we used this technique to analyze the uptake of ARS-TiO_2 nanoconjugates in the human cell lines PC-3M and MCF-7[29]. Here, we investigated the uptake of ARS-TiO_2 in whole organisms (i.e., in Arabidopsis seedlings). ARS, an anthraquinone derivative (Figure 1A) chelates calcium, magnesium, barium, strontium and iron, and has been widely used for the fluorescent labeling of calcium deposits in animals and occasionally for the detection of localized calcium accumulates in plants. [32, 33] Because the same vicinal hydroxyl groups of ARS (Figure 1A) which chelate calcium are the ones that bind Ti on the surface of nanoparticulate TiO_2, ARS bound to NPs becomes an integral part of the nanoconjugate (NC) and it is not expected to interact with inorganic calcium. [29, 33] As anticipated [29], conjugation of 50 or 100% of the total surface of Ti atoms with ARS (TiO_2-ARS) caused a visible red shift in the absorbance of NCs in the UV spectral range, and a broad absorption peak between 400 nm and 550 nm (Figure 1B-C). Moreover, sucrose coating of TiO_2 NPs

also caused a red shift, forming a larger area below the curve at wavelengths below 350 nm (Figure 1C). Nevertheless, the absorbance of sucrose-coated NPs after addition of ARS once again shows the same pattern as the absorbance of NPs exposed to ARS alone (Figure 1C). This occurs because the binding affinity of surface Ti atoms for ARS as a bidentate ligand is stronger than their affinity for sucrose, a linear carbon molecule with hydroxyl groups.

Unlike animal cells, plant cells are surrounded by an extra barrier, the cell wall, with pores that are believed to be in the 5 – 20 nm diameter range. [34, 35] Given the size of the TiO_2 NCs used in this study, we expected that the cell wall would not prevent diffusion of NCs towards the plasma membrane. To establish a fast and reproducible method for the application of TiO_2-ARS NCs, we compared the staining of plants that were either grown on agar-containing Murashige and Skoog media (MS/2 [36]) supplemented with NCs, or grown on MS/2 media and then incubated in water containing a nonionic surfactant (0.1% Triton X-100) and NCs. The bare and sucrose-coated TiO_2-50% ARS NCs did not affect the germination and growth of plants sown on MS/2 media with a concentration-range from 0.1 μM to 10 μM NCs. We also did not observe any visible uptake of TiO_2-ARS NCs by the germinating seedlings (data not shown). Considering the complex chemical structure of the agar polysaccharides, this was not an entirely unexpected result; the NCs are likely retained in the agar-containing media in the same way as they are retained in agarose gels. [25, 30] Next, we stratified seeds for 1 to 10 days in a 10 μM aqueous solution of bare and sucrose-coated TiO_2-50% ARS NCs, and followed the effects of this treatment by analyzing the staining of the embryo, the seed germination index, and the size and ARS staining of the germinated seedlings. We observed no uptake of either bare or sucrose-coated TiO_2-50% ARS NCs in the embryonic cells, and no effect on the seed germination index even after a 10-day-long stratification in the presence of NCs (data not shown). Most of the TiO_2-50% ARS NCs remained bound to the seed mucilage and after prolonged incubation they precipitated in the media or around the seed (Figure 2). This suggests that seed mucilage may offer a strong protection to the embryo from TiO_2 NPs present in the environment.

Next, we tested how five-day-old, MS/2 media-grown Col-0 seedlings stained in a 0.1% Triton X-100 solution containing a sonicated suspension of bare or sucrose-coated TiO_2-50% ARS NCs. While Degussa TiO_2 NPs are known to be photocatalytic and generate free radicals in aqueous media[37] and 8-hydroxy-2-deoxyguanosine in DNA[38], this activity depends on the absorption of photons of energy greater than 3.2 eV in the UV light range (λ=338 nm) by the TiO_2. However, the conjugation of ARS accompanied by a red shift of the semiconductor UV-VIS absorption spectra (Figure 1C) leads to a decrease of the semiconductor band gap, and excitation at visible light wavelengths. To avoid needless injury to the plants that can be induced by photocatalytic activity of NCs, we first determined the doses of TiO_2-ARS NCs that led to a visible staining of seedlings after 24 hrs of incubation at 22 °C in the dark. Subsequently, within that dose range we tested the production of free radical species in whole seedlings (Figure 3). Incubation with 0.5 μM, 1 μM and 5 μM of bare or sucrose-coated TiO_2-50% ARS NCs visibly stained the primary roots (Figure 3A). The staining was less intense in plants incubated with sucrose-coated NCs than in plants incubated with bare NCs (e.g., compare 0.5 μM dose in Figure 3A). To detect the production of superoxide radical ($O_2^{\cdot -}$), nitroblue tetrazolium (NBT) at a final concentration of 0.05% was added directly to the incubation medium, and vacuum infiltrated into seedlings for 30 min in the dark. Seedlings were then fixed in 100% ethanol and analyzed by bright-field microscopy. At the sites of $O_2^{\cdot -}$ production, NBT is reduced and precipitates as blue formazan. [39] We observed no formazan crystal formation in the cotyledons even with the highest dose of TiO_2-50% ARS NCs (data not shown). Similarly, root cells that were intensely stained with TiO_2-ARS NPs also did not accumulate formazan, suggesting that even at 5 μM, the NPs do not impose an excessive oxidative stress on the root tissues (Figure 3B).

Bright-field microscopic analyses of Arabidopsis seedlings treated with 1 μM of sucrose-coated TiO_2-50% ARS NCs showed that the intense root staining ends at the hypocotyl-root junction i.e., at the boundary between the aerial and subterranean plant organs (Figure 4A). The surface of the roots from the root tips to the hypocotyls-root junction was covered in TiO_2-ARS NC aggregates (Figure 3B and Figure S3 in Supporting Information). In contrast, NC aggregates were not observed around the hypocotyls and leaves, although the entire seedlings were submerged in the NC suspension during the treatment (data not shown and Figure 3). The accumulation of ZnO and carbon NPs at the root surface has been described previously [9, 12, 15], but the underlying mechanism has not been discussed. We propose that the accumulation of TiO_2-50% ARS NC aggregates at the root surface area is the result of H^+ extrusion by root cells. Roots of all plants export H^+ to promote the uptake of micronutrients from the environment, resulting in a low pH in the area surrounding any root. [40] This increase in H^+ concentration is expected to cause the acid-catalyzed enolization of the carbonyl groups of ARS and the subsequent cross-linking of neighboring NCs through their attached ARS molecules, leading to the accumulation of NC aggregates around the roots. Because our studies have been conducted in vitro, it remains to be shown whether the aggregation of NPs and NCs also occurs around the roots of soil-grown plants, and whether this reduces the uptake of nanostructures from the environment into plants and thus, NP and NC entry into the food chain. Despite some loss due to their aggregation at the root surface, a substantial portion of NCs entered the Arabidopsis root. At a macroscopic examination, the staining of roots was obvious after 6 hrs of incubation with TiO_2-ARS NCs, and it increased with time (Figure S3A in Supporting Information, and Figure 4B). For all further experiments, we chose to analyze samples that were stained for 24 hrs. At this time point, we detected the characteristic TiO_2-ARS NCs red stain in all root cell types except the cells of the root cap and the lateral root primordia (Figure S3B and S3C in Supporting Information). Parallel studies with ARS alone showed a different staining pattern and a different shade of red (red for NCs and magenta for ARS alone; Figures 3A, 4B, 5A, 5B and S3). In root cells, NCs accumulated in the nuclei and vacuoles (Figure 4C, and Figures S3C and S3D in Supporting Information).

For some of the potential applications of NPs in plants, such as the nano-harvesting and isolation of polyphenols and other secondary metabolites that accumulate in leaves, the localization of NCs in shoot organs is of more interest than root uptake. After 24 hrs incubation with sucrose-coated TiO_2-50% ARS NCs, we detected intensely stained vesicles in the epidermal pavement cells, intensely stained bodies in the kidney-shaped stomatal guard cells, and a more diffuse staining in palisade cells (Figure 5). Treatment with ARS alone did not lead to any accumulation of the dye in epidermal cells, while the palisade cells stained diffusely (Figure 5A and B). The TiO_2-50% ARS NCs-stained organelles in stomatal guard cells resembled central vacuoles. [41] Vacuoles of guard cells are dynamic structures that regulate guard cell volume and thus, the size of the stomatal pore and transpirational water loss. [42] To confirm that the vacuoles of the adaxial guard cells have the shape and size suggested by the TiO_2-ARS NCs accumulation pattern, we incubated seedlings in 0.1% Triton X-100 with neutral red (NR), an acidotropic dye which accumulates in the vacuolar lumen and endosomes.[43] Indeed, the NR stain also accumulated in the kidney-shaped bodies in stomatal guard cells (Figure 5C). Independent of the duration of the NC treatment, only a fraction of stomata accumulated TiO_2-50% ARS NCs, and this was not correlated with their position on the cotyledon (Figure 5A). It has been shown previously that 43 ± 6 nm fluorescent polystyrene particles with carboxylate-modified surfaces penetrate into the stomatal pore, but no uptake was detected in the guard cells or the surrounding epidermal cells. [44] Interestingly, this study also showed that only some of the stomata accumulated NPs in their pores, and their position on the leaf seemed random. The significance of these findings is currently unknown.

The second type of intense epidermal staining with TiO_2-50% ARS NCs were the spherical bodies in pavement cells of cotyledons and epidermal cells of hypocotyls and petioles (Figure 5A and D, and Figure S4 in Supporting Information). Because a similar pattern was observed after staining with the vacuole and endosome-staining NR, we concluded that these organelles are endosomes (Figure 4D). A recent study with positively charged 1 nm-large gold NPs described the localization of NPs in early and late endosomes of tobacco protoplasts, and showed that the NPs are internalized both by clathrin-dependent and independent endocytic pathways. [16] Because the gold study was conducted on protoplasts and ours on intact plants, we concluded that the cell walls are indeed not a barrier for the cellular uptake of TiO_2 NCs smaller than 5 nm which were used in this study. In addition, the subcellular distribution of NCs in foliar cells suggests the involvement of both endocytotic and stomatal foliar uptake pathways.

Finally, and as a confirmation that the red staining in stomatal guard cells derives from TiO_2-ARS NCs, we have sectioned frozen O.C.T. (Optimal cutting temperature compound, Tissue-Tek, Sakura Finetek, Torrance, CA, USA)-embedded plants, and placed the 10 micron thick sections on silicon nitride (Si_3N_4) windows for X-ray fluorescence microscopy (XFM). Visible light microscopy of one section of cotyledons revealed the characteristic shape of stomata (data not shown); that position was recorded, and XFM was performed as described previously. [28, 29] Elemental maps were acquired by XFM on beamline 2-ID-E at the Advanced Photon Source, and confirmed the enrichment of Ti and therefore NCs in stomatal guard cells (Figure 6). The localized, punctuated Ti signals of variable strengths detected in subsidiary cells (i.e., anatomically distinct epidermal cells that surround the stomatal guard cells, and together with guard cells form the stomatal apparatus) probably correspond to the endosomes noted with optical microscopy (Figure 5 and Figure S4 in Supporting Information). The maps of natural plant elements Cl, P, Mn and Zn outlined plant cells by their 2D distribution, with most of the elements being present at equal amounts in guard and subsidiary cells (Figure 6A). The only exception was Cu which showed the highest accumulation in one of the guard cells. Elemental concentrations of different pixels in micrograms/cm^2 were as follows: Cl (0-3.14), P (0-2.65), Mn (0-0.27), Cu (0-1.23), and Zn (0-1.5). Ti concentrations of different pixels varied between 0 and 1.17 micrograms/cm^2. However, the map distribution of Ti overlapped the best with the stomatal guard cells and punctuate “hot spots” in the subsidiary cells (Figure 6B). When Ti concentration values were recalculated on a per volume basis, and the size of NPs taken into consideration, we found that each guard cell contained about $(25.26 \pm 0.01) \times 10^8$ NP, while each “hot spot” contained $(0.94 \pm 0.01) \times 10^8$ NP. Additional sections of cotyledons showed a similar elemental distribution pattern (data not shown).

To summarize, ARS-functionalized ultra-small TiO_2 NCs were able to move into Arabidopsis seedlings where they displayed a distinct distribution pattern. This work has addressed several essential questions in plant nanobiology: (1) are ultra-small anatase TiO_2 NPs capable of passing the cell walls of plant cells; (2) are these nanoconjugates capable to penetrate deeper into the plant tissues-beyond the surface cell layers; and (3) are there tissue- and cell-specific distributions of such NPs in intact plants. In this study, we have shown that intact plants incubated with TiO_2 internalize nanoparticles, and that these particles can be seen throughout the plant body. Moreover, we learned that the internalized nanoparticles localize in a number of cellular compartments. Combined, these data suggest that ARS-TiO_2 nanoconjugates can be used for uptake and distribution studies in plants.

This study offers to the plant community a critical new insight and opens at least three areas of future research. First, the finding that NCs enter into intact plant cells, despite the cell wall, will facilitate confocal microcopy-based uptake and localization studies similar to those conducted in animal cells[29]. This will remove uncertainties stemming from the use of

protoplasts, and will allow large scale comparisons of available Arabidopsis mutant lines. Second, the frequent presence of NCs in the nuclei of root cells suggests that anatase TiO_2-ARS NCs can be used for the efficient delivery of short oligonucleotides or peptides to this subcellular location. This, in turn, may lead to the development of new methods for suppressing gene function in the Arabidopsis root. Modifications of NPs with organelle targeting peptides or oligonucleotides, similar to those used in mammalian cells, [25, 28] may lead to the development of a novel set of tools for *Arabidopsis* engineering. Finally, the vacuolar localization of TiO_2 NCs in leaves opens up the possibility of exploiting the NP surface affinity of anatase TiO_2 for enediol ligands to selectively harvest polyphenols and other plant natural products stored in the central vacuoles.

Supplementary Material

Refer to Web version on PubMed Central for supplementary material.

Acknowledgments

We are grateful to Tara L. Burke for performing the seed germination assays, AiGuo Wu for instructions on nanoparticle synthesis and characterization, Katarina Petras for nanoparticle sizing assistance, Lenell Reynolds and Northwestern Cell Imaging Facility for assistance with TEM and Dr. Lydia Finney with assistance in beamline setup. This work was supported in part by NIH grant EB002100-03. Use of the Advanced Photon Source at Argonne National Laboratory was supported by the U. S. Department of Energy, Office of Science, Office of Basic Energy Sciences, under Contract No. DE-AC02-06CH11357.

REFERENCES

1. Pérez-de-Luque A, Rubiales D. Pest. Manag. Sci. 2009; 65(5):540–545. [PubMed: 19255973]
2. Torney F, Trewyn BG, Lin VS, Wang K. Nat. Nanotechnol. 2007; 2(5):295–300. [PubMed: 18654287]
3. Asli S, Neumann PM. Plant Cell Environ. 2009; 32(5):577–584. [PubMed: 19210640]
4. Corredor E, Testillano PS, Coronado M, González-Melendi P, Fernández-Pacheco R, Marquina C, Ricardo Ibarra M, de la Fuente JM, Rubiales D, Pérez-de-Luque A, Risueño M. BMC Plant Biol. 2009; 9:45. [PubMed: 19389253]
5. González-Melendi P, Fernández-Pacheco R, Coronado MJ, Corredor E, Testillano PS, Risueño MC, Marquina C, Ibarra MR, Rubiales D, Pérez-De-Luque A. Ann. Bot. 2008; 101(1):187–195. [PubMed: 17998213]
6. Lee W, An Y, Yoon H, Kweon H. Environ. Toxicol. Chem. 2008; 27(9):1915–1921. [PubMed: 19086317]
7. Lin D, Xing B. Environ. Pollut. 2007; 150:243–250. [PubMed: 17374428]
8. Lin D, Xing B. Environ. Sci. Technol. 2008; 42(15):5580–5585. [PubMed: 18754479]
9. Lin S, Reppert J, Hu Q, Hudson JS, Reid ML, Ratnikova TA, Rao AM, Luo H, Ke PC. Small. 2009; 5(10):1128–1132. [PubMed: 19235197]
10. Marshall AT, Haverkamp RG, Davies CE, Parsons JG, Gardea-Torresdey JL, van Agterveld D. Int. J. Phytoremediat. 2007; 9(1-3):197–206.
11. Monica RC, Cremonini R. Caryologia. 2009; 62(2):161–165.
12. Wild E, Jones KC. Environ. Sci. Technol. 2009; 43(14):5290–5294. [PubMed: 19708355]
13. Yang L, Watts DJ. Toxicol. Lett. 2005; 158(2):122–132. [PubMed: 16039401]
14. Zheng L, Hong F, Lu S, Liu C. Biol. Trace Elem. Res. 2005; 104(1):83–92. [PubMed: 15851835]
15. Zhu H, Han J, Xiao JQ, Jin Y. J. Environ. Monitor. 2008; 10(6):713–717.
16. Onelli E, Prescianotto-Baschong C, Caccianiga M, Moscatelli A. J. Exp. Bot. 2008; 59(11):3051–3068. [PubMed: 18603619]
17. Su M, Liu J, Yin S, Ma L, Hong F. Biol. Trace Elem. Re.s. 2008; 124(2):173–183.
18. Lei Z, Mingyu S, Xiao W, Chao L, Chunxiang Q, Liang C, Hao H, Xiaoqing L, Fashui H. Biol. Trace Elem. Res. 2008; 121(1):69–79. [PubMed: 18186002]

19. Hong F, Yang F, Liu C, Gao Q, Wan Z, Gu F, Wu C, Ma Z, Zhou J, Yang P. Biol. Trace Elem. Res. 2005; 104(3):249–260. [PubMed: 15930594]
20. Monteiller C, Tran L, MacNee W, Faux S, Jones A, Miller B, Donaldson K. Occup. Environ. Med. 2007; 64(9):609–615. [PubMed: 17409182]
21. Suh WH, Suslick KS, Stucky GD, Suh Y-H. Prog. Neurobiol. 2009; 87(3):133–170. [PubMed: 18926873]
22. Initiative AG. Nature. 2000; 408(6814):796–815. [PubMed: 11130711]
23. Alonso JM, Stepanova AN, Leisse TJ, Kim CJ, Chen H, Shinn P, Stevenson DK, Zimmerman J, Barajas P, Cheuk R, Gadrinab C, Heller C, Jeske A, Koesema E, Meyers CC, Parker H, Prednis L, Ansari Y, Choy N, Deen H, Geralt M, Hazari N, Hom E, Karnes M, Mulholland C, Ndubaku R, Schmidt I, Guzman P, Aguilar-Henonin L, Schmid M, Weigel D, Carter DE, Marchand T, Risseeuw E, Brogden D, Zeko A, Crosby WL, Berry CC, Ecker JR. Science. 2003; 301(5633): 653–657. [PubMed: 12893945]
24. Y., L.; Last, RL. The Arabidopsis Book. The American Society of Plant Biologists; 2009. Web-based Arabidopsis functional andstructural genomics resources.; p. 1-14.
25. Paunesku T, Rajh T, Wiederrecht G, Maser J, Vogt S, Stojicevic N, Protic M, Lai B, Oryhon J, Thurnauer M, Woloschak G. Nat. Mater. 2003; 2(5):343–346. [PubMed: 12692534]
26. Rabatic BM, Dimitrijevic NM, Cook RE, Saponjic ZV, Rajh T. Adv. Mate.r. 2006; 18(8):1033–1037.
27. Rajh T, Chen L, Lukas K, Liu T, Thurnauer MC, Tiede DM. J. Phys. Chem. B. 2002; 106(41): 10543–10552.
28. Paunesku T, Vogt S, Lai B, Maser J, Stojicevic N, Thurn KT, Osipo C, Liu H, Legnini D, Wang Z, Lee C, Woloschak GE. Nano Lett. 2007; 7(3):596–601. [PubMed: 17274661]
29. Thurn KT, Paunesku T, Wu A, Brown EMB, Lai B, Vogt S, Maser J, Aslam M, Dravid V, Bergan R, Woloschak GE. Small. 2009; 5(11):1318–1325. [PubMed: 19242946]
30. Brown EM, Paunesku T, Wu A, Thurn KT, Haley B, Clark J, Priester T, Woloschak GE. Anal. Biochem. 2008; 383(2):226–235. [PubMed: 18786502]
31. Wu AG, Paunesku T, Brown EMB, Babbo A, Cruz C, Aslam M, Dravid V, Woloschak GE. NANO. 2008; 3(1):27–36. [PubMed: 19890457]
32. Geisler-Lee J, Gallie DR. Plant Physiol. 2005; 139(1):204–212. [PubMed: 16126861]
33. Puchtler H, Meloan SN, Terry MS. J. Histochem. Cytochem. 1969; 17(2):110–124. [PubMed: 4179464]
34. Rondeau-Mouro C, Defer D, Leboeuf E, Lahaye M. In.t J. Biol. Macromol. 2008; 42(2):83–92.
35. Carpita N, Sabularse D, Montezinos D, Delmer DP. Science. 1979; 205(4411):1144–1147. [PubMed: 17735052]
36. Kurepa J, Toh-e A, Smalle J. Plant J. 2008; 53:102–114. [PubMed: 17971041]
37. Xia T, Kovochich M, Brant J, Hotze M, Sempf J, Oberley T, Sioutas C, Yeh JI, Wiesner MR, Nel AE. Nano Lett. 2006; 6(8):1794–1807. [PubMed: 16895376]
38. Zhu RR, Wang SL, Chao J, Shi DL, Zhang R, Sun XY, Yao SD. Mater. Sci. Eng., C. 2009; 29(3): 691–696.
39. Dunand C, Crevecoeur M, Penel C. New Phytol. 2007; 174(2):332–341. [PubMed: 17388896]
40. Monshausen GB, Bibikova TN, Messerli MA, Shi C, Gilroy S. Proc. Natl. Acad. Sci. USA. 2007; 104(52):20996–21001. [PubMed: 18079291]
41. Tanaka Y, Kutsuna N, Kanazawa Y, Kondo N, Hasezawa S, Sano T. Plant Cell Physiol. 2007; 48(8):1159–1169. [PubMed: 17602189]
42. MacRobbie E. Proc. Natl. Acad. Sci. USA. 2000; 97(22):12361–12368. [PubMed: 11027317]
43. Dubrovsky JG, Guttenberger M, Saralegui A, Napsucialy-Mendivil S, Voigt B, Baluska F, Menzel D. Ann. Bot. 2006; 97(6):1127–1138. [PubMed: 16520341]
44. Eichert T, Kurtz A, Steiner U, Goldbach HE. Physiol. Plant. 2008; 134:151–160. [PubMed: 18494856]
45. Arsovski AA, Villota MM, Rowland O, Subramaniam R, Western TL. J. Exp. Bot. 2009; 60(9): 2601–2612. [PubMed: 19401413]

46. Western TL, Skinner DJ, Haughn GW. Plant Physiol. 2000; 122(2):345–356. [PubMed: 10677428]

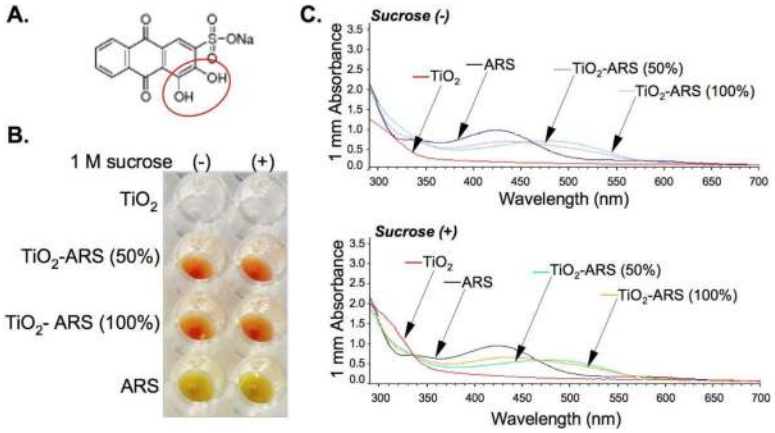

Figure 1. Functionalization of 2.8 ± 1.4 nm TiO_2 NPs with Alizarin red S

A. Structure of Alizarin red S (ARS; 4-dihydroxy-9,10-dioxo-2-anthracenesulfonic acid, sodium salt). The vicinal hydroxyl groups expected to bind to TiO_2 NPs are circled.

B. Appearance of the TiO_2 NP suspensions after coating with ARS. The NPs (20 μM with a surface site molarity of 4.11 mM) were dialyzed against 10 mM sodium phosphate pH 5.7 (Sucrose (-)). After dialysis in phosphate buffer, an aliquot of NP suspension was dialyzed against 1M sucrose in 10 mM sodium phosphate pH 5.7 (Sucrose (+)). Dialyzed NPs (surface site molarity of 4.11 mM) were mixed with 4 mM ARS (in 10 mM sodium phosphate pH 5.7) to yield either 50% or 100% ARS coated NCs.

C. UV-VIS absorbance spectra of TiO_2 NPs, ARS, and TiO_2-ARS NCs. Both bare (Sucrose (-)) and sucrose-coated (Sucrose (+)) NCs do not absorb light at wavelengths above 350 nm. ARS alone (4 mM) has an absorbance peak at 420 nm. The absorbance peak of ARS-coated TiO_2 NCs is red-shifted.

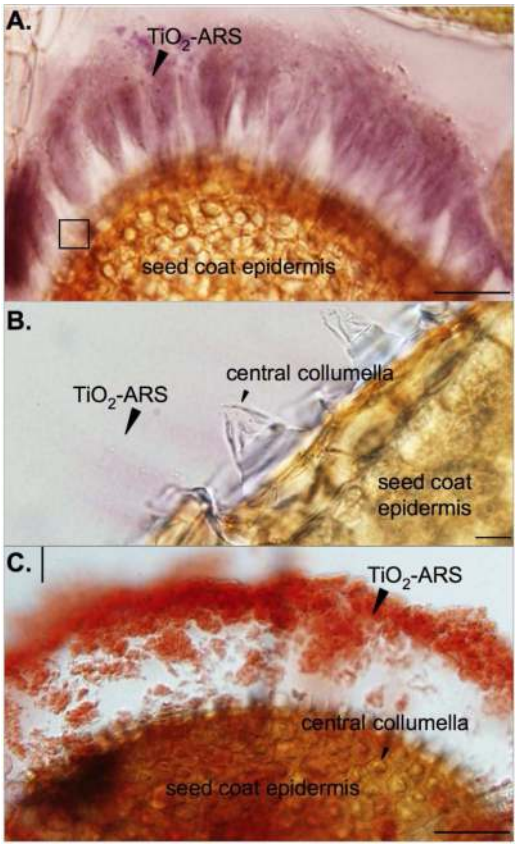

Figure 2. Treatments of seeds with TiO_2-50% ARS nanoconjugates

Seeds were imbibed in 1 μM TiO_2-50% ARS NCs at 4°C for 24 hrs (A and B) or 7 days (C). The region boxed in A is shown under higher magnification in B. The seed coat (*testa)* protects the plant embryo. The seed coat epidermal cells contain mucilage, and have thick radial cell walls and central pyramidal elevations known as columellae. When seeds are exposed to water, the hydrophilic mucilage of the epidermal cells instantly hydrates, which leads to rupture of the cell wall and the release of mucilage which forms a pectin hydrogel capsule surrounding the seed. [45, 46] *Arabidopsis* seed mucilage is primarily composed of rhamnogalacturonan I. [45, 46] The large arrowheads point to the accumulation of NCs in seed mucilage. The small arrowheads point to the central columella. Scale bar in A and C: 100 μm and scale bar in B: 10 μm.

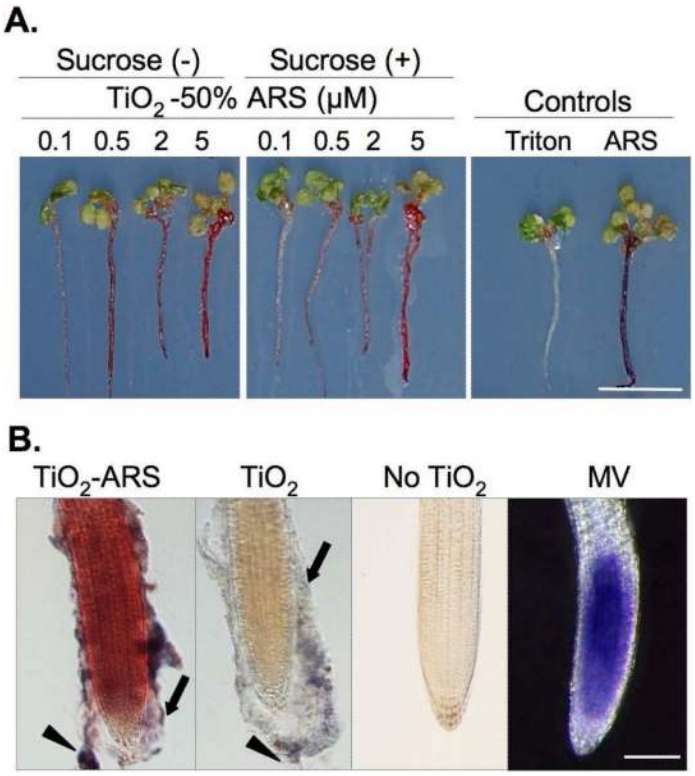

Figure 3. Nanoconjugate uptake in five-day-old Arabidopsis seedlings

A. Plants were grown on vertically positioned MS/2 plates and transferred to incubation media (0.1% Triton X-100) containing the denoted doses of NCs. Representative seedlings were photographed after a 24 hour-long incubation. Plants incubated in 0.1% Triton X-100 (Triton) or 0.1% Triton X-100 supplemented with 5 μM ARS are shown as controls.

B. Root tips of representative seedlings incubated for 24 hrs with 5 μM sucrose-coated TiO_2-50% ARS NCs (TiO_2-ARS) or 5 μM sucrose-coated non-modified TiO_2 NPs, and post-stained with NBT. Blue formazan crystals (arrows) are formed around NPs coating the root (arrowheads), but no formazan precipitate was detected in the root tip cells. Root tip of a seedling incubated for 24 hrs in 0.1% Triton X-100 (no TiO_2) and root tip of a seedling incubated for 24 hrs with the superoxide-generating compound methyl viologen (MV, 100 μM) are shown as negative and positive controls, respectively.

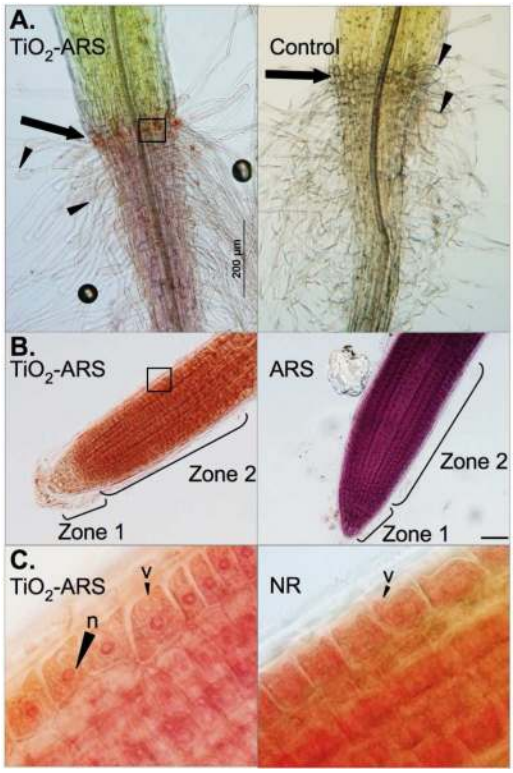

Figure 4. Root uptake of sucrose-coated TiO_2-50% ARS nanoconjugates in five-day-old Arabidopsis seedlings

A. Zone encompassing the hypocotyl-root junction (arrow) of representative seedlings treated with 1 μM sucrose-coated TiO_2-50% ARS NCs (TiO_2-ARS) or with a Triton X-100 (Control) solution. Arrowheads point to swollen root hairs. The square accents the base of root hairs in which NCs accumulated. The high-magnification micrograph of this region is shown as Figure S2 in Supporting Information. The Triton X-100 control shows that swollen root hairs are an artifact of the incubation/sample preparation procedures, and not a result of NC toxicity. Scale bar: 200 μm.

B. Primary root tips of representative seedlings incubated one day in 1 μM sucrose-coated TiO_2-50% ARS NCs (TiO_2-ARS) or in 1 μM ARS. Zone 1 encompasses the columella and lateral root cap and zone 2 corresponds to the root meristem. The region squared in the micrograph of TiO_2-50% ARS NCs-treated seedlings is shown enlarged in C. Scale bar: 100 μm.

C. Higher magnification micrograph of the area squared in B shows that sucrose-coated TiO_2-50% ARS NCs accumulate in nuclei (n, large arrowheads) and vacuoles (v, small arrowheads) of root cells. In parallel, seedlings were stained with 0.01% neutral red in 80 mM sodium phosphate buffer, pH 7.2 (NR) to show the position and size of the vacuoles (v, arrowhead) in the root cells in Zone 2. Scale bar: 50 μm.

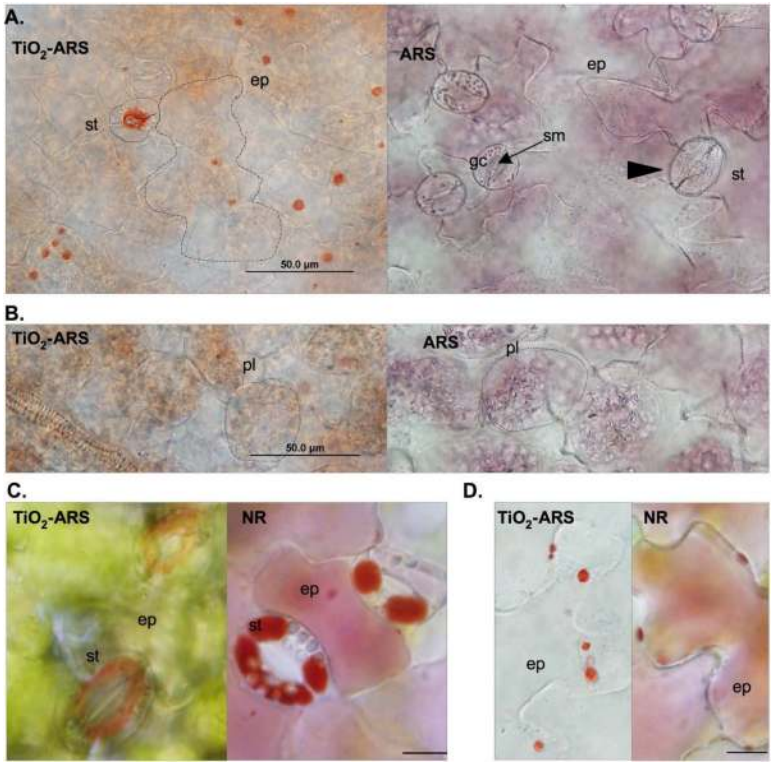

Figure 5. Foliar uptake of sucrose-coated TiO_2-50% ARS nanoconjugates

A. Micrographs of adaxial cotyledonary epidermis of five-day-old seedlings incubated with 1 μM TiO_2-50% ARS NCs (TiO_2-ARS) or 1 μM ARS. Stomata (st) with stomatal guard cells (gc) and stomatal mouth (sm) and pavement cells (ep) are outlined. Scale bar: 50 μm.

B. Subepidermal layer of cotyledons of five-day-old seedlings incubated with 1 μM TiO_2-50% ARS NCs (TiO_2-ARS) or 1 μM ARS. Palisade mesophyll cells (pl) are outlined. Scale bar: 50 μm.

C. Frontal view of the stomatal apparatus (st) of cotyledons in seedlings incubated in 1 μM TiO_2-50% ARS NCs (TiO_2-ARS) or 0.01% neutral red in 80 mM sodium phosphate buffer, pH 7.2 (NR). ep, epidermal cells. Scale bar: 10 μm.

D. Micrograph of the adaxial epidermal pavement cells (ep) of five-day-old cotyledons stained with 1 μM TiO_2-50% ARS NCs (TiO_2-ARS) or NR. Scale bar: 10 μm.

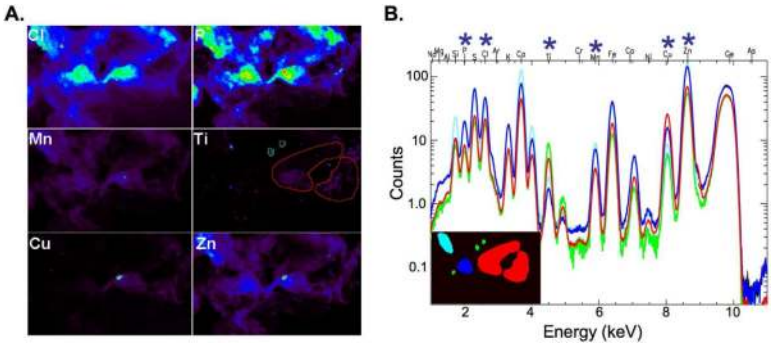

Figure 6. X-ray fluorescence microscopy of the region around an adaxial stoma from the cotyledon stained with sucrose-coated TiO_2-50% ARS nanoconjugates

A. XFM of a ten micron thick section of an Arabidopsis cotyledon shows elemental two-dimensional maps for Ti from nanoconjugates and for the naturally occurring elements Cl, P, Mn, Cu and Zn. Scanning was done in raster mode over an area of 60 by 120 microns; each pixel was 1 micron square. Maps show the shape of the two stomatal guard cells (outlined in red in the Ti map) and the surrounding epidermal cells. Ti "hot spots" corresponding to the endosomes in epidermal cells are outlined in green. Elements are indicated by white letters in the upper right corner of each map. In these false color images red indicates the strongest signal (highest elemental concentration) and black the lowest. **B.** Complete elemental spectra obtained by averaging pixel values over the area covered by the two guard cells (red), Ti "hot spots" (green) or two other areas (light and dark blue). Elemental differences between these different regions of interest are such that for most elements, as well for Ti, guard cells and "hot spots" cluster together.